Scientific paper

Surfactant Assisted Sonochemical Synthesis and Characterization of Gadolinium Doped Zinc Oxide Nanoparticles

Heena Khajuria, Jigmet Ladol, Rajinder Singh, Sonika Khajuria and Haq N. Sheikh*

Post-Graduate Department of Chemistry, University of Jammu, Baba Sahib Ambedkar Road, Jammu Tawi, 180006 India

** Corresponding author: E-mail: hnsheikh@rediffmail.com*
Tel.: +91-191-2493124 Fax: +91-191-2431365

Received: 24-03-2015

Abstract

Pure and Gd doped Zinc Oxide (ZnO) nanoparticles were synthesized by sonochemical method using different surfactants (PVP/CTAB). The nanoparticles were characterized by powder X-ray diffraction (PXRD), Fourier transform infrared spectroscopy (FTIR), scanning electron microscopy (SEM), energy dispersive X-ray spectroscopy (EDS), particle size analysis by DLS technique and UV-Visible spectroscopy. The effect of Gd doping and nature of surfactants on crystallite size, morphology and band gap of ZnO nanoparticles have been investigated. In addition to this, the effect of nature of surfactant on amount of dopant inserted in the ZnO lattice was also studied.

Keywords: Polyvinylpyrrolidone; cetyltrimethyl ammonium bromide; ultrasonic synthesis

1. Introduction

Nanosized semiconductors have attracted extensive interest due to their unique properties and applications.[1–3] A lot of research work has been done in the synthesis and characterization of semiconducting nanostructures such as ZnO, ZnS, PbS, CdS, CdSe and TiO_2.[4–8] ZnO is one of these semiconductor materials which have great potential for applications in photocatalysis, solar cells, chemsensors, transducers, transparent electrodes, electroluminescent devices and ultraviolet laser diodes. The applications of ZnO are because of its novel properties such as direct wide band gap (3.37 eV), optical transparency and large exciton binding energy (60 meV) that ensures significant excitonic emission at room temperature. In addition, ZnO is inexpensive and environmental friendly as compared to other metal oxides. The properties and applications of ZnO can be improved by modulating its bandgap[9] and controlling its morphology and particle size.[10] This can be achieved by doping of selective elements into ZnO. Doping induces drastic changes in its optical, electrical and magnetic properties by modifying its electronic structure.[11–13] Different methods have been used for the synthesis of doped ZnO such as laser ablation,[14] magneton sputtering,[15] high temperature calcinations,[16] sol-gel,[17] hydrothermal[18] and sonochemical methods[19]. Among these techniques, sonochemical method has attracted much attention.[20–22] It is based on acoustic cavitation resulting from the continuous formation, growth and implosive collapse of bubbles in a liquid.[23] It has become one of the useful, green, simple and fast methods for the synthesis as well as doping of nanostructures.

Till now, number of studies on various transition (Fe, Co, Mn etc.) and inner transition metal ions (Er, Nd, Ce, La, Eu, etc.)-doped ZnO have been reported.[24–31] Lanthanide ions are considered as excellent candidates as dopant of the ZnO due to their many optical and magnetic advantages. Gd is recognized as a potential dopant and has become the focus of numerous investigations because of its promising applications in optoelectronic and magnetic devices.[32]

Here, we report synthesis of Gd doped ZnO with varying dopant concentration (0.5 mol%, 1.0 mol%, 1.5 mol%, 2.0 mol%) by sonochemical method. The synthesis of nanoparticles was carried out in the presence of

surfactants namely polyvinylpyrollidone (PVP) and cetyltrimethyl ammonium bromide (CTAB). Surfactants have the ability to control the morphology[33] and size distribution of nanoparticles[34] and it has been found that surfactants also control the concentration of dopant inserted into the host lattice. Hence, the effect of these additives (PVP and CTAB) and that of concentration of dopant (Gd^{3+}) on particle size, morphology, and optical properties of ZnO nanoparticles was investigated by means of different techniques such as XRPD, FT-IR, EDS, SEM and UV-Visible spectroscopy and particle size analysis.

2. Experimental

2. 1. Materials

All reagents used for the synthesis were commercially available and used as received. Zinc acetate and cetyltrimethyl ammonium bromide were purchased from Acros. Polyvinylpyrrolidone was purchased from Sigma Aldrich and gadolinium nitrate was purchased from Alfa Aesar. Doubly distilled water was used to prepare aqueous solutions.

2. 2. Synthesis

To prepare undoped ZnO nanoparticles, 50 mL aqueous solution of (0.10 M, 1.09 g) zinc acetate and surfactant PVP/CTAB (0.5 g) was prepared. The mixture was positioned in a high intensity ultrasound probe and sonicated for 30 min. Aqueous solution of ammonia (5%) was slowly added in the above sonicated solution. In this step, nano-structured zinc hydroxide was formed.

$$Zn(CH_3COO)_2(aq) + 2\,NH_4OH \rightarrow \rightarrow Zn(OH)_2(s) + 2CH_3COONH_4(aq) \quad (1)$$

At the end of process of adding ammonia solution, the mixture was sonicated for 1 h. The precipitated zinc hydroxide was filtered and washed with distilled water and ethanol. The precipitates were dehydrated at 320 °C for 2 h in air.

$$Zn(OH)_2(s) \rightarrow ZnO(s) + H_2O(g) \quad (2)$$

During dehydration, nanostructured zinc oxide was formed. The nanoparticles were sonicated in ethanol for 30 min to eliminate agglomeration, centrifuged and dried at 70 °C in air. Gd^{3+} doped zinc oxide were obtained under the similar conditions by replacing a fraction of $Zn(CH_3COO)_2$ by $Gd(NO_3)_3$ (0.011 g), (0.022 g), (0.034 g) and (0.045 g) for 0.5 mol%, 1.0 mol%, 1.5 mol%, and 2 mol% doping respectively). The scheme of the synthetic procedure of Gd doped ZnO is presented in the Figure 1.

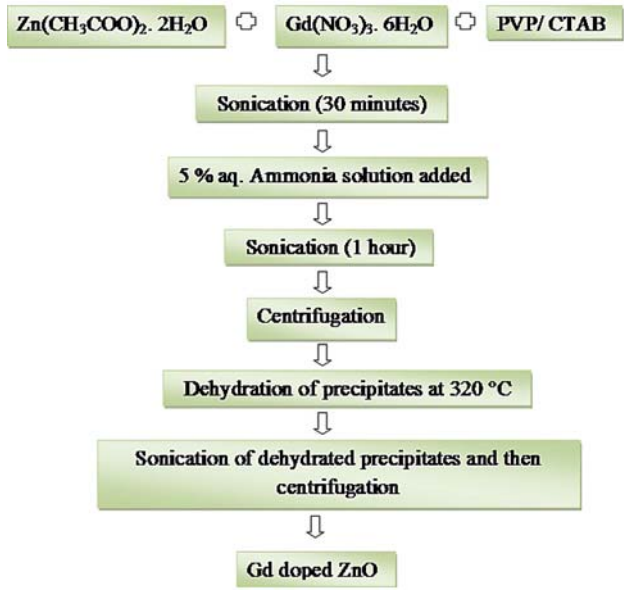

Figure 1. Flowchart of synthetic procedure of Gd doped ZnO.

2. 3. Characterization

The crystalline phase structure and size of the products were determined from X-ray powder diffraction (XRPD) using Panalytical X'pert-Pro diffractometer system in the 2θ range from 10° to 80° with Cu Kα radiation (λ = 1.5418 Å). The morphology of the as prepared samples was observed using scanning electron microscope (Quanta 200 3D) equipped with EDS measurement. The UV-Visible absorption spectra of the samples were recorded on T90+ UV/Vis Spectrophotometer (PG instruments Ltd). The FT-IR spectra of the prepared samples were recorded by using Shimadzu Prestige-21 infra-red spectrophotometer. The particle size of the samples was determined by the dynamic light scattering (DLS) technique using a Zetasizer nano ZS 90, Malvern make. All the measurements were performed at room temperature.

3. Results and Discussion

3. 1. Infrared Spectroscopy

FT-IR spectra of prepared undoped and Gd doped ZnO nanoparticles were recorded in the range of

Table 1. IR frequency shift of Zn–O stretching frequency under the influence of Gd doping.

Sample	PVP	CTAB
	υ(Zn–O) /cm^{-1}	
Undoped ZnO	480	482
0.5 mol% Gd: ZnO	455	474
1.0 mol% Gd: ZnO	449	447
1.5 mol% Gd: ZnO	446	435
2.0 mol% Gd: ZnO	445	430

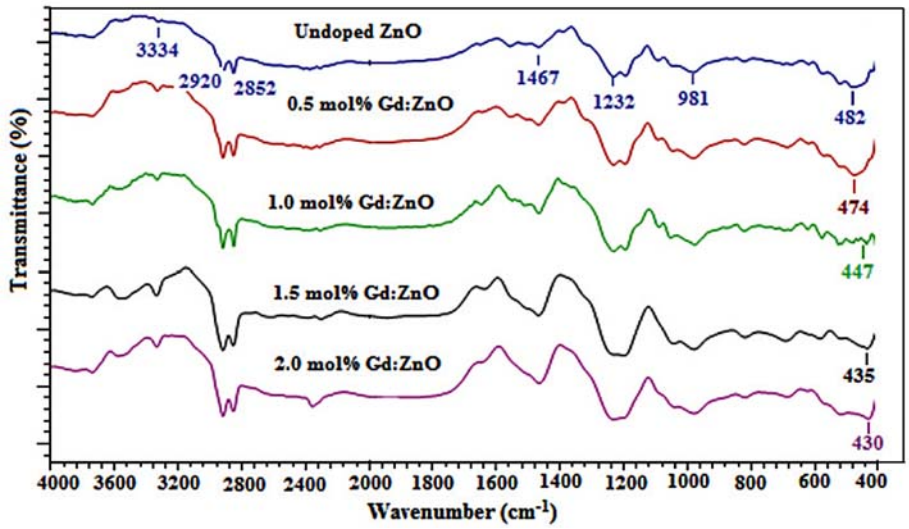

Figure 2a. FT-IR spectra of undoped and Gd doped ZnO nanoparticles synthesized using CTAB.

4000–400 cm^{-1}. Figures 2a and 2b show the IR spectra of undoped and Gd doped ZnO nanoparticles prepared in presence of CTAB and PVP respectively.

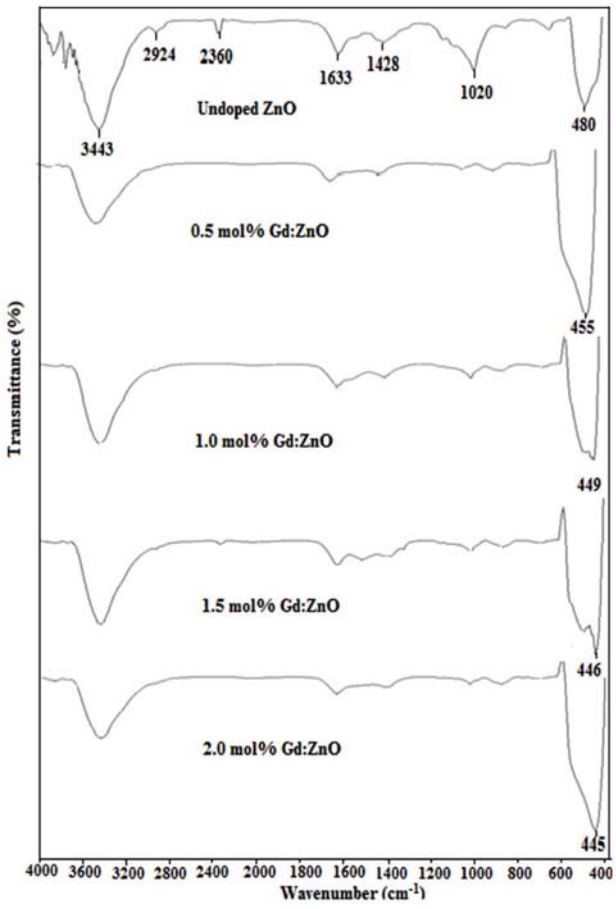

Figure 2b. FT-IR spectra of undoped and Gd doped ZnO nanoparticles synthesized using PVP.

The FT-IR spectra of samples show a prominent and characteristic absorption band in the range of 450–500 cm^{-1}. This band is attributed to the stretching modes of Zn-O bond. This characteristic absorption undergoes red shift on doping with Gd^{3+} (Table 1) which indicates that the Zn-O-Zn network is perturbed by the presence of Gd^{3+} in its environment. This means that Zn–O bond strength decrease and/or bond length increases with increase in the concentration of dopant. A few absorption peaks were also observed between 900 and 2900 cm^{-1} in all samples. Absorption peaks around 980–1050 cm^{-1} is assigned to C–C stretching mode of the acetate groups. The peaks around 1400–1600 cm^{-1} are attributed to the C–O stretching modes (symmetric and asymmetric) and peaks around 2800–2900 cm^{-1} are attributed to C–H bond of the acetate group. A broad band near 3400 cm^{-1} is assigned to stretching vibrations of the O–H group of H_2O molecules adsorbed on the surface of ZnO nanoparticles. The above result, therefore, suggest attachment of hydroxy (–OH) and acetate (CH_3COO) groups on the surface of undoped and Gd doped ZnO nanoparticles.

3. 2. Powder X-Ray Diffraction

Figure 3 (a, b) display XRPD patterns of the undoped and Gd doped ZnO nanoparticles prepared in CTAB and PVP medium respectively. In both cases, the diffraction peaks for samples doped with Gd corresponds to hexagonal wurtzite ZnO as reported in JCPDS card no. 36–1451, and no detectable diffraction peak for any impurity phase such as Gd_2O_3, Gd $(OH)_3$, Gd metal or Gd-Zn alloy was found. This indicated that the Gd^{3+} ions substituted Zn sites without changing the wurzite crystal structure of ZnO and without any precipitated phase or clustering. However, the diffraction peaks shift to lower angle slightly as dopant concentration (Gd) increases from

0.5–2.0 mol%, indicating that the lattice parameters get changed when Gd^{3+} are incorporated into ZnO lattice.

Table 2. Crystallite size of undoped and Gd doped ZnO calculated by Williamson-Hall method.

Sample	CTAB *D* /nm	PVP *D*/nm
Undoped ZnO	56	52
0.5 mol% Gd: ZnO	51	46
1.0 mol% Gd: ZnO	46	41
1.5 mol% Gd: ZnO	42	39
2.0 mol% Gd: ZnO	40	33

This is due to the reason that the ionic radius of Gd^{3+} (R = 0.94 Å) is bigger than that of Zn^{2+} (R = 0.74 Å).

It is noted that the full width at half maximum (FWHM) of the diffraction peaks of ZnO changes with change in concentration of dopant (Gd^{3+}) and nature of surfactants.[35] This affect on the crystallite size of undoped and doped ZnO nanoparticles is estimated from XRD data by using Williamson-Hall method.[36] The crystallite size of the doped ZnO nanoparticles is found to be smaller than undoped ZnO nanoparticles (Table 2). It may be due to the decrease in grain growth of Gd doped ZnO nanoparticles as compared to pure ZnO nanoparticles. The crystallite size of the nanoparticles is controlled by the rate of grain

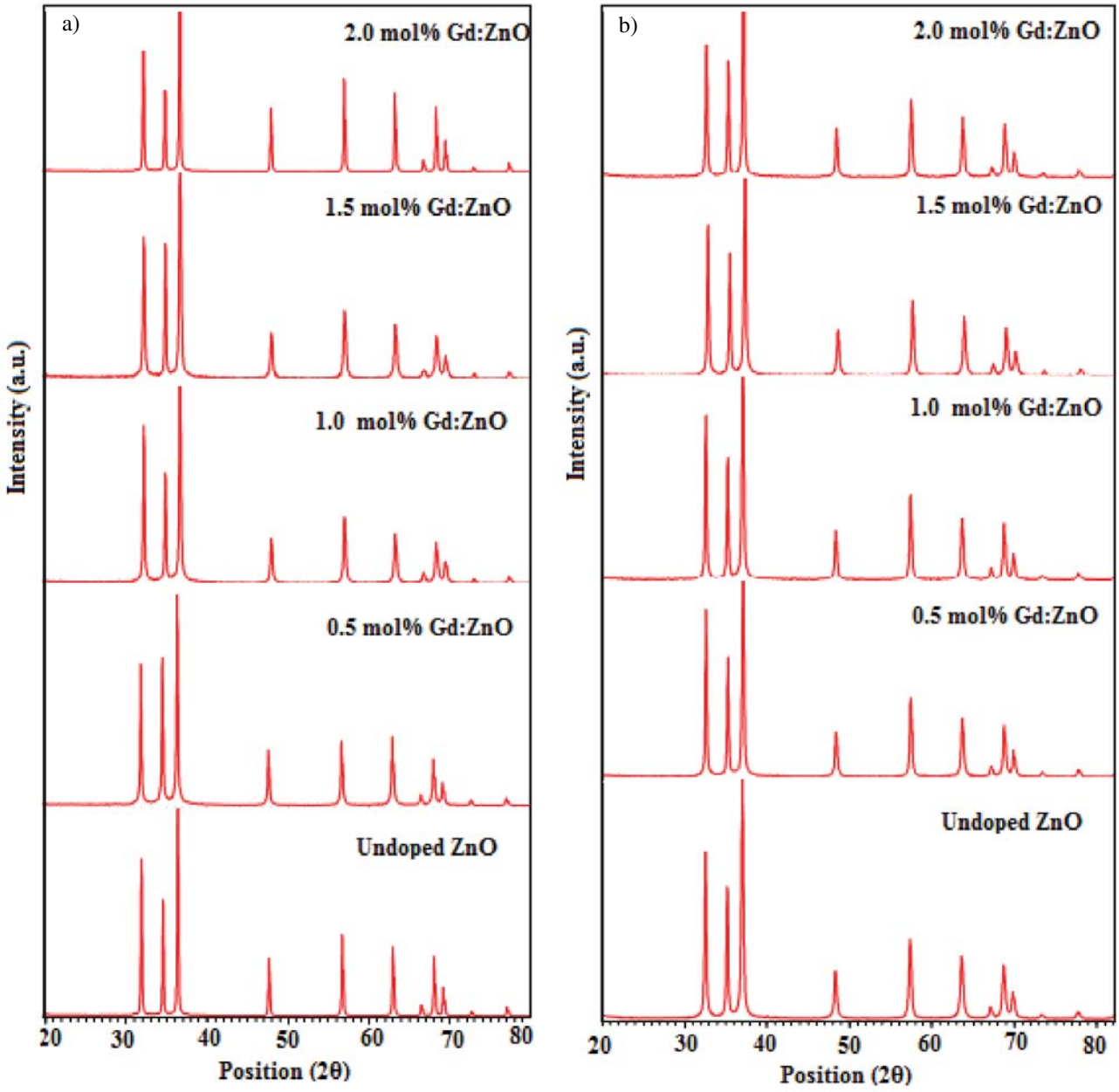

Figure 3. PXRD pattern of undoped and Gd doped ZnO nanoparticles synthesized using (a) CTAB and (b) PVP.

growth which in turn depends upon movement of grain boundaries. The growth of the crystal grains can be prevented by resisting the motion of grain boundaries. Smaller crystallite sizes of doped nanoparticles suggest the presence of secondary phase or impurity (dopant) as a main reason for preventing the motion of grain boundaries and thus growth of doped ZnO nanoparticles.[37]

3. 3. Scanning Electron Microscopy

The surface morphology of the Gd^{3+} doped ZnO nanoparticles (CTAB/PVP) was examined with scanning electron microscope. SEM micrographs of Gd^{3+} doped ZnO (CTAB) show nanorods and flowerlike nanostructures (Figure 4(a–c). However, SEM micrographs of Gd^{3+}

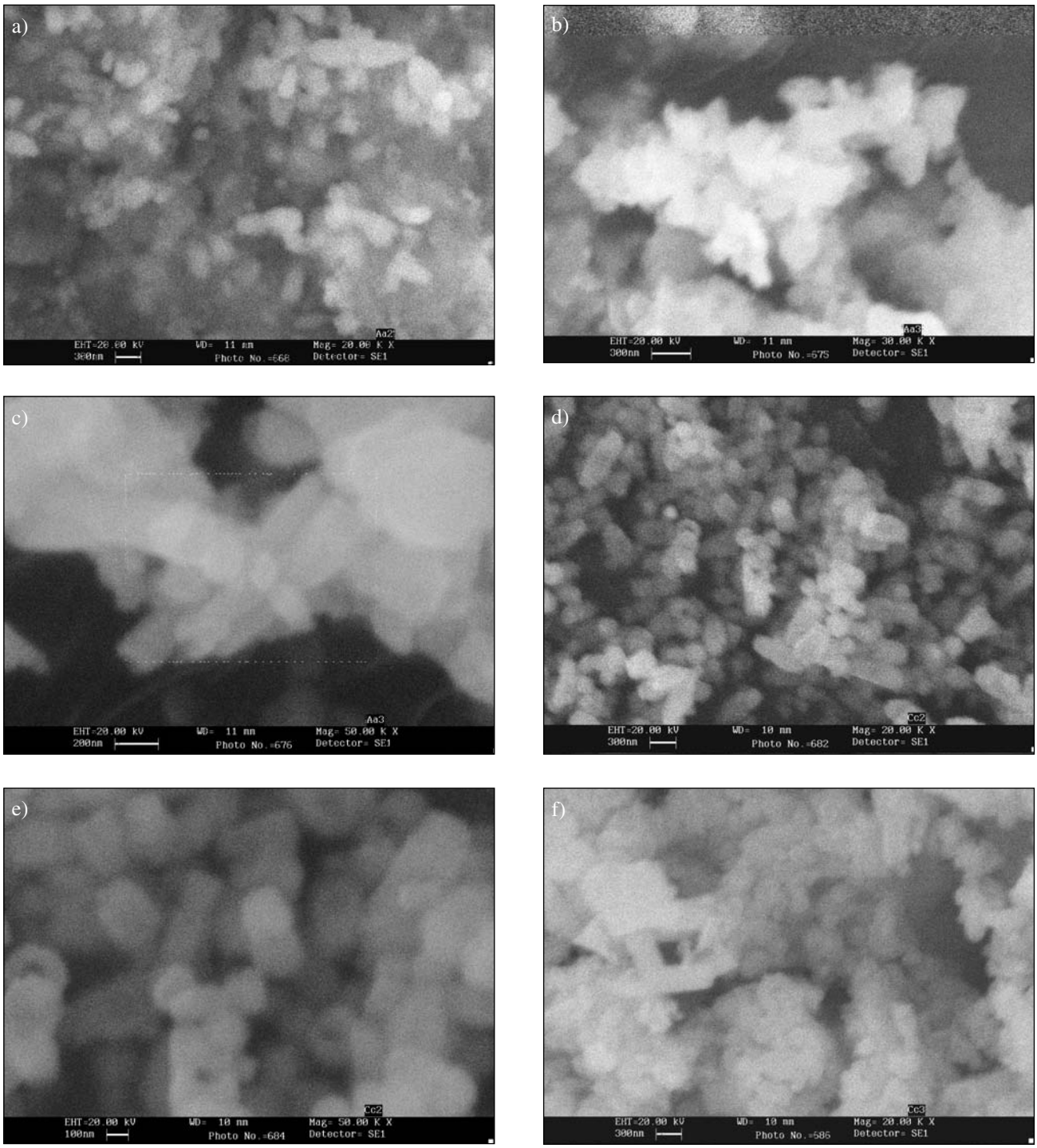

Figure 4. SEM micrographs of (a) 1.0 mol% Gd doped ZnO (CTAB) (b, c) 1.5 mol% Gd doped ZnO (CTAB) (d, e) 1.0 mol% Gd doped ZnO (PVP) (f) 1.5 mol% Gd doped ZnO (PVP).

doped ZnO nanoparticles (PVP) show clusters of spherical shaped particles (Figure 4 (d–f). The results suggest that surfactants can control the morphology of particles. The aggregation of the particles increases with increase in the dopant concentration.

3. 4. Energy Dispersive X-Ray Spectroscopy

EDS was performed to investigate the presence and concentration of dopant in the doped ZnO nanoparticles. Figure 5(a–d) show energy dispersive X-ray spectra of Gd doped ZnO covered over width of 23nm . The results confirm that prepared Gd doped ZnO (CTAB/PVP) nanoparticles are assuredly composed of Gd, Zn, and O. Atomic ratios of Zn : O : Gd in 1.0 and 1.5 mol% Gd: ZnO (CTAB/PVP) are given in Table 3. In general, lesser amount of Gd was found in the doped samples than provided in the precursor solution. This indicates that there are some hindrances during incorporation of the dopant into the host lattice. This may be because of the large difficulties associated with the doping of rare earth ions into the ZnO host. Firstly, the ionic radii of RE ions (e.g., Gd^{3+} = 0.94 Å) are much larger than that of the Zn^{2+} ion (0.74 Å); and secondly, the substitution creates a charge imbalance, as RE^{3+} ions (charge: +3) substitute the Zn^{2+} sites (charge: +2) in the ZnO host matrix. Moreover, in the presence of different surfactants, the amount of dopant incorporated into the ZnO host is different for same concentration of doping. Higher amount of dopant is found in the ZnO lattice prepared in presence of PVP as compared to that of CTAB (Table 3). Thus, nature of surfactant has effect on the concentration of dopant incorporated in the host lattice. The elemental mapping of doped samples shows that Gd is uniformly distributed without any embedded nanoclusters (Figure 6).

Table 3. Weight and Atomic percentage of Zn, O, and Gd in Gd doped ZnO NPs calculated from EDS spectra.

	CTAB				PVP			
Elements	**1.0 mol% Gd: ZnO**		**1.5 mol% Gd: ZnO**		**1.0 mol% Gd: ZnO**		**1.5mol% Gd: ZnO**	
	Wt. %	**At. %**	**Wt. %**	**At. %**	**Wt.%**	**At. %**	**Wt. %**	**At. %**
Zn	78.03	54.70	79.01	57.63	79.68	61.61	80.59	64.85
O	15.11	43.30	13.44	40.08	11.22	35.47	9.70	31.90
Gd	6.85	2.00	7.55	2.29	9.10	2.92	9.71	3.25

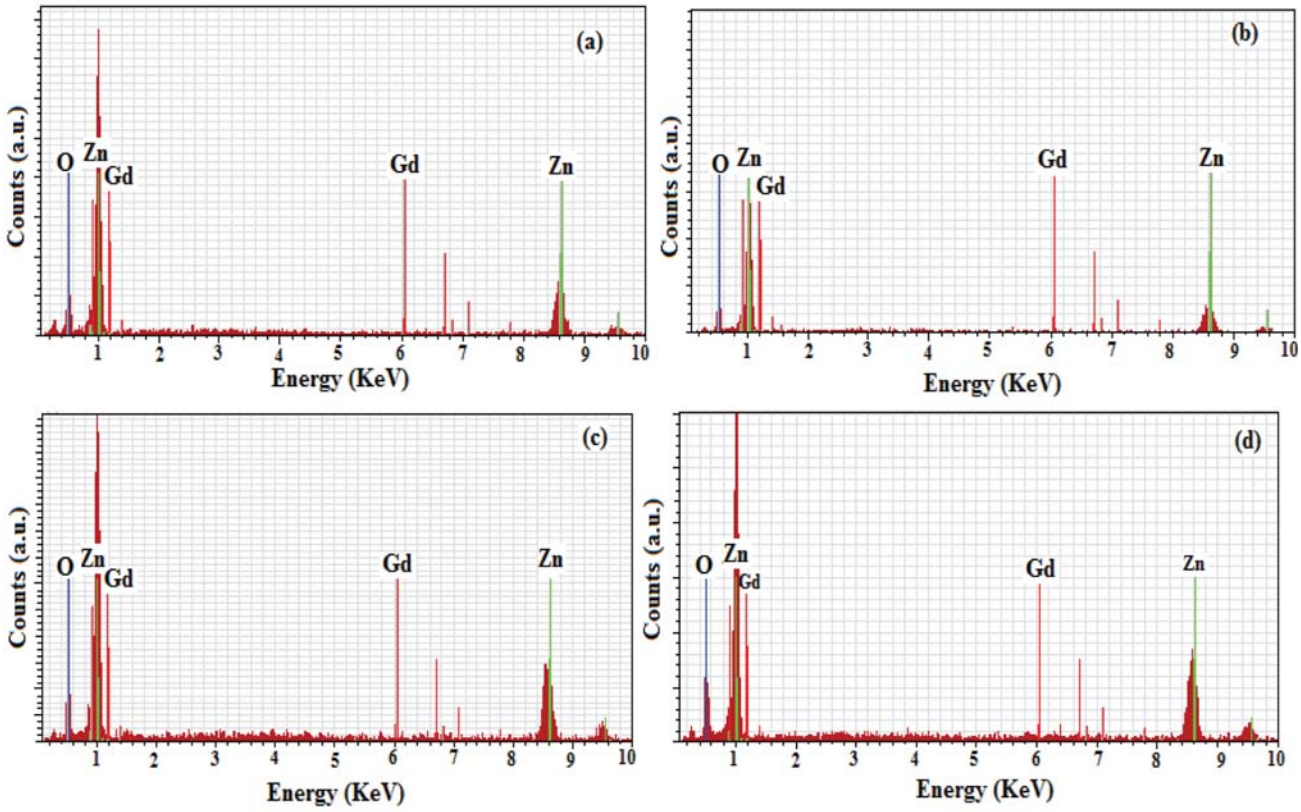

Figure 5. EDS spectra of (a) 1.0 mol% Gd doped ZnO (CTAB) (b) 1.5 mol% Gd doped ZnO (CTAB) (c) 1.0 mol% Gd doped ZnO (PVP) (d) 1.5 mol% Gd doped ZnO (PVP).

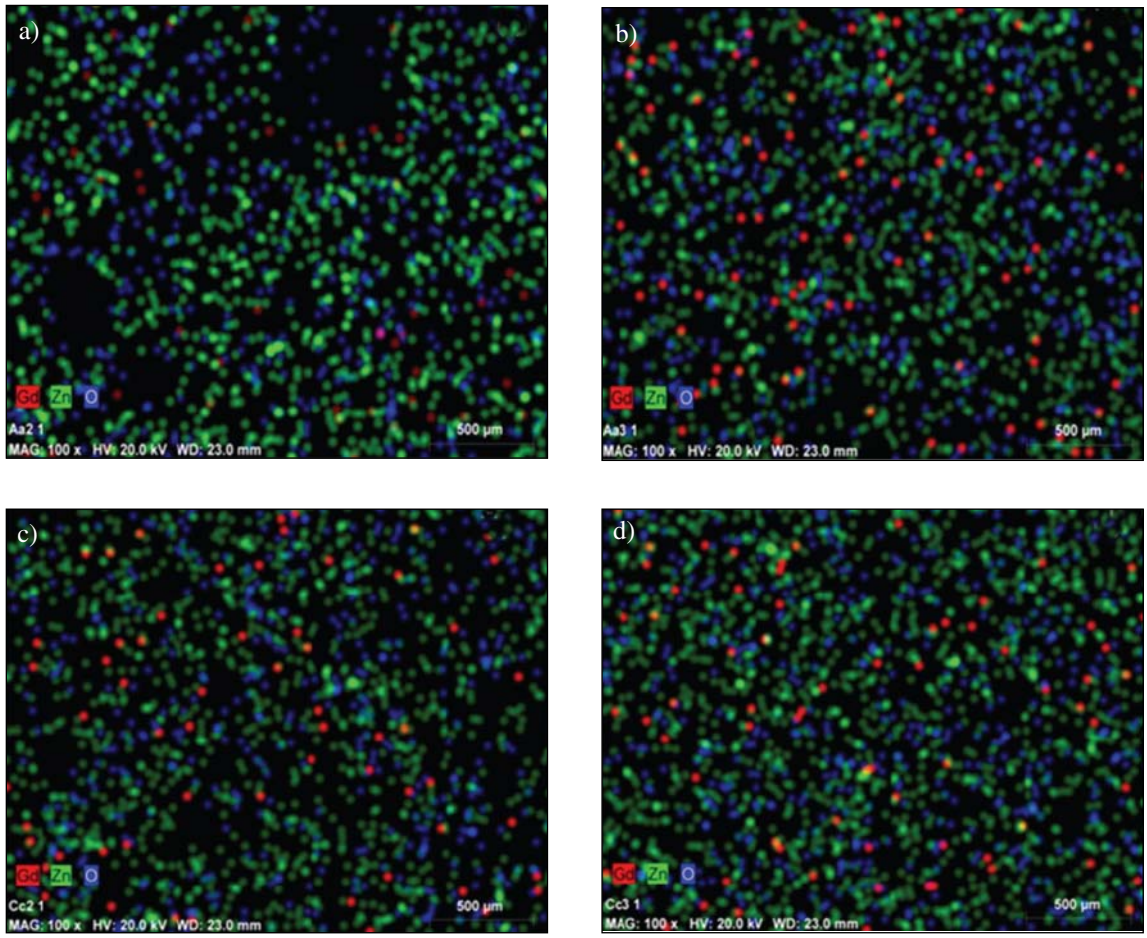

Figure 6. Elemental mapping of (a) 1.0 mol% Gd doped ZnO (CTAB) (b) 1.5 mol% Gd doped ZnO (CTAB) (c) 1.0 mol% Gd doped ZnO (PVP) (d) 1.5 mol% Gd doped ZnO (PVP).

3. 5. Particle Size Analysis by Dynamic Light Scattering Technique

The particle size distributions of the synthesized undoped and Gd doped ZnO nanoparticles (CTAB/PVP) were studied by dynamic light scattering technique. The average particle size distribution of synthesized undoped and doped ZnO is presented in Figure 7. The nanoparticles were uniformly dispersed in aqueous medium by mild sonication for 10 min before DLS analysis. The approximate size of

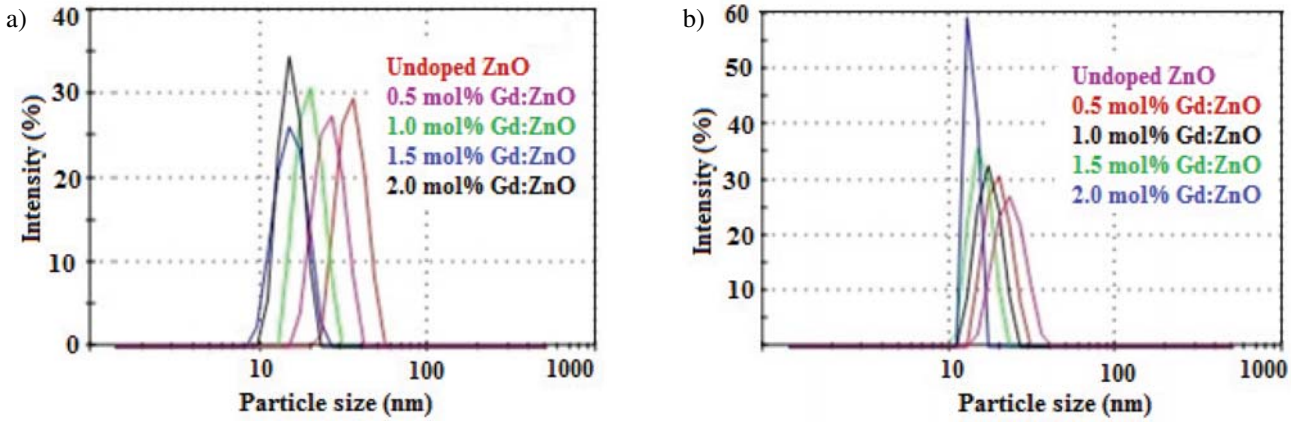

Figure 7. Particle size distribution of undoped and Gd doped ZnO nanoparticles synthesized using (a) CTAB and (b) PVP.

undoped ZnO nanoparticles is found to be 50 nm and 38 nm for CTAB and PVP medium respectively. The particle size of doped nanoparticles decreases with increase in the concentration of dopant. The particle size of the product obtained in the presence of PVP is smaller than that in CTAB.

3. 6. UV-Visible Spectroscopy

The optical property and band gap of surfactant (PVP /CTAB) assisted undoped and Gd doped nanoparticles were studied using absorption spectra. The UV-Vis spectra of undoped and doped ZnO samples are shown in Figure 8. The PVP and CTAB assisted undoped ZnO shows an absorption peak at 379 nm and 369 nm respectively, which undergoes red shift on doping with Gd. The absorption refers to the transition of electrons from the valence band to conduction band and band gap is the energy difference (in electron volts) between the top of the valence band and the bottom of the conduction band in semiconductors. The optical bandgap of the undoped and doped ZnO was calculated using equation:

Table 4. Absorption wavelength and calculated bandgap of undoped and Gd doped ZnO.

Sample	CTAB		PVP	
	λ/nm	E_g/eV	λ/nm	E_g/eV
Undoped ZnO	369	3.36	379	3.27
0.5 mol% Gd: ZnO	372	3.33	380	3.26
1.0 mol% Gd: ZnO	375	3.30	385	3.22
1.5 mol% Gd: ZnO	381	3.25	386	3.21
2.0 mol% Gd: ZnO	383	3.2	395	3.13

$$E_g = hc/\lambda = 1240/\lambda \quad (3)$$

where E_g is the bandgap in eV, λ is the wavelength in nm.

The calculated band gaps for the Gd-doped ZnO samples are given in Table 4 and it is observed that band gap decreases with increase in the concentration of dopant which is due to the fact that dopant ions introduce new electronic levels inside the ZnO band gap.

3. 7. Effect of Nature of Surfactant on Doping

Surfactants affect the stoichiometric composition and morphology of nanoparticles. A surfactant molecule has a hydrophilic head and a long hydrophobic tail. The overall mechanism of action of surfactant system is such that their molecules embrace the crystals and control their excess growth. CTAB is a cationic surfactant with positively charged head and a long hydrophobic tail. In CTAB solution, the zinc acetate molecules come closer to the positively charged micellar head region due to the electrostatic interactions between the head groups of cationic micelles and negatively charged acetate groups of zinc acetate which result in localization of the zinc acetate precursor on the micellar surface. Thus, the micellar surface becomes the preferred reaction site for the formation of the intermediate. However, positively charged CTAB head region may inhibit the approach of Gd^{3+} ions on the surface of ZnO intermediate due to electrostatic repulsion, thus less amount of dopant was inserted in the CTAB assisted doped ZnO. In case of PVP, the polyvinyl backbone serves as a hydrophobic group whereas the pyrrolidone

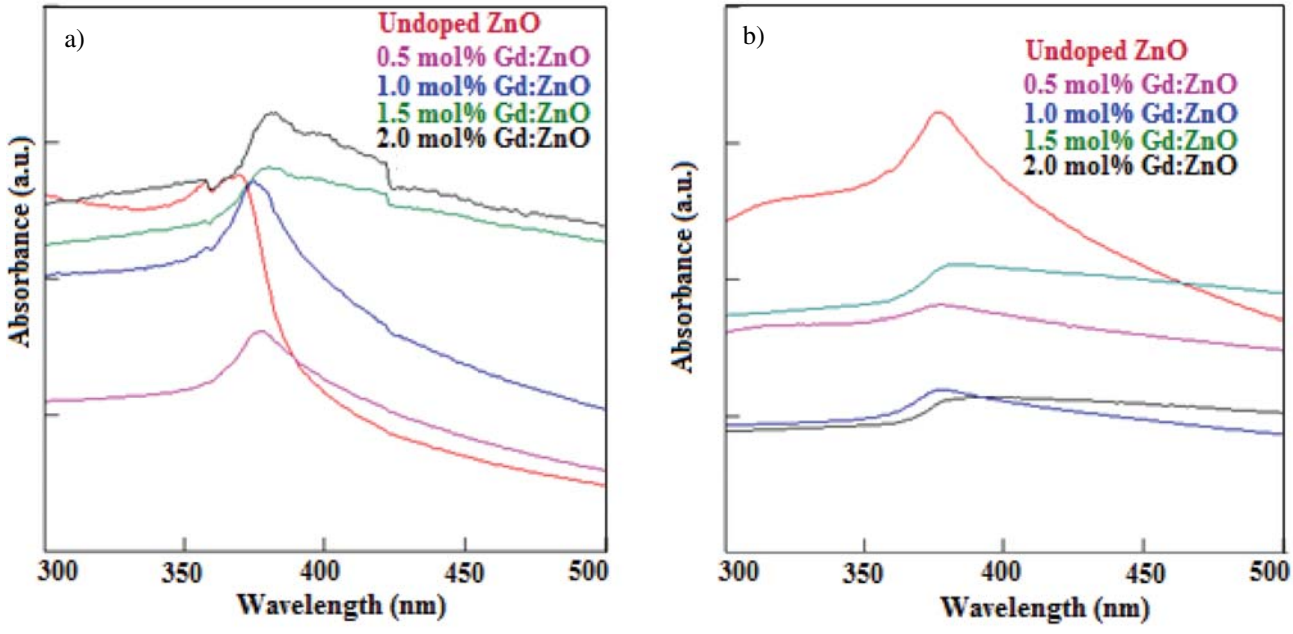

Figure 8. UV- Vis spectra of undoped and Gd doped ZnO nanoparticles synthesized using (a) CTAB and (b) PVP.

group serves as a hydrophilic group. The carbonyl functional groups of PVP coordinate onto the Zn^{2+} ions of intermediate surfaces. A coordinative bonding of CO to Zn^{2+} at the ZnO/PVP interface may form. Gd^{3+} ions also have coordinative interaction to CO of PVP so that they may be absorbed on the surface of intermediate through PVP. Thus, in this case comparatively high amount of dopant (Gd) is incorporated into the host lattice.

4. Conclusions

Pure and Gd doped ZnO nanoparticles were prepared by sonochemical method in the presence of surfactants (PVP & CTAB). XRPD studies confirmed the hexagonal wurtzite structure for all the samples. The presence of Gd ions within the ZnO lattice was confirmed by XRPD and FT-IR study. The microstructure analysis showed the different morphology for doped ZnO samples prepared in CTAB and PVP. The effect of nature of surfactants on doping was investigated by EDS studies which clearly showed that higher amount of dopant were inserted in the ZnO lattice in case of PVP than CTAB. UV-Visible spectroscopy indicated that the band gap for Gd doped ZnO nanoparticles decreases with an increase in Gd-doping as compared to pure ZnO.

5. References

1. A. M. Smith, S. Nie, *Acc. Chem. Res*. **2010**, *43*, 190–200. http://dx.doi.org/10.1021/ar9001069
2. J. Liqiang, S. Xiaojun, S. Jing, C. Weimin, X. Zili, D. Yaoguo, F. Honggang, *Sol. Energy Mater. Sol. Cells* **2003**, *79*, 133–151. http://dx.doi.org/10.1016/S0927-0248(02)00393-8
3. H. Karami, M. Ghasemi, S. Matini, *Int. J. Electrochem. Sci*. **2013**, *8*, 11661–11679.
4. P. Rodriguez-Fragoso, J. Reyes-Esparza, A. Leon-Buitimea, L. Rodriguez-Fragoso, *J. Nanobiotechnology* **2012**, *10*, 1–11. http://dx.doi.org/10.1186/1477-3155-10-47
5. H. M. Chen, C. K. Chen, R. -S. Liu, L. Zhang, J. Zhang, D. P. Wilkinson, *Chem. Soc. Rev.* **2012**, *41*, 5654–5671. http://dx.doi.org/10.1039/c2cs35019j
6. J. Tian, Z. Zhao, A. Kumar, R. I. Boughton, H. Liu, *Chem. Soc. Rev*. **2014**, *43*, 6920–6937. http://dx.doi.org/10.1039/C4CS00180J
7. D. Sarkar, C. K. Ghosh, K. K. Chattopadhyay, *Cryst. Eng. Comm.* **2012,** *14*, 2683–2690. http://dx.doi.org/10.1039/c2ce06392a
8. C. H. Chang, H. Jung, Y. Rheem, K. -H. Lee, D. -C. Lim, Y. Jeong, J. -H. Lim, N. V. Myung, *Nanoscale* **2013,** *5*, 1616–1623. http://dx.doi.org/10.1039/c2nr33029f
9. Y. Wang, Y. Yang, X. Zhang, X. Liu, A. Nakamurab, *Cryst. Eng. Comm.* **2012,** *14*, 240–245. http://dx.doi.org/10.1039/C1CE05733B
10. N. Talebian, S. M. Amininezhad, M. Doudi, *J. Photochem. Photobiol. B* **2013**, *120*, 66–73. http://dx.doi.org/10.1016/j.jphotobiol.2013.01.004
11. Y. Yang, H. Lai, H. Xu, C. Tao, H. Yang, *J. Nanopart. Res*. **2010**, *12*, 217–225. http://dx.doi.org/10.1007/s11051-009-9598-x
12. S. H. Deng, M. Y. Duan, M. Xu, L. He, *Physica B* **2011,** *406*, 2314–2318. http://dx.doi.org/10.1016/j.physb.2011.03.067
13. J. Hays, K. M. Reddy, N. Y. Graces, M. H. Engelhard, V. Shutthanandan, M. Luo, C. Xu, N. C. Giles, C. Wang, S. Thevuthasan, A. Punnoose, *J. Phys.: Condens. Matter* **2007,** *19*, 1–24. http://dx.doi.org/10.1088/0953-8984/19/26/266203
14. S. Harako, S. Yokoyama, K. Ide, X. Zhao, S. Komoro, *Phys. Stat. Sol. (a)* **2008,** *205*, 19–22. http://dx.doi.org/10.1002/pssa.200776709
15 H. Chen, J. Ding, F. Shi, Y. Li, W. Guo, J. Alloys Compd. **2012**, *534,* 59–63. http://dx.doi.org/10.1016/j.jallcom.2012.04.064
16. R. Krishna, D. Haranath, S. P. Singh, H. Chander, A. C. Pandey, D. Kanjilal, *J. Mater Sci.* **2007**, *42*, 10047–10051. http://dx.doi.org/10.1007/s10853-007-2053-4
17. M. K. Lima, D. M. Fernandes, M. F. Silva, M. L. Baesso, A. M. Neto, G. R. Morais, C. V. Nakamura, A. O. Caleare, A. A. W. Hechenleitner, E. A. G. Pineda, *J. Sol-Gel Sci. Technol* **2014,** *72*, 301–309. http://dx.doi.org/10.1007/s10971-014-3310-z
18. P. Yu, J. Wang, H. -Y. Du, P. -J. Yao, Y. Hao, X. -G. Li, *J. Nanomater* **2013**, *2013*, 1–6.
19. A. Phuruangrat, O. Yayapao, T. Thongtem, S. Thongtem, *J. Nanomater.* **2014**, *2014*, 1–9.
20. J. H. Bang, K. S. Suslick, *Adv. Mater*. **2010,** *22*, 1039–1059. http://dx.doi.org/10.1002/adma.200904093
21. A. Khataee, A. Karimi, S. A. Oskoui, R. D. C. Soltani, Y. Hanifehpour, B. Soltani, S. W. Joo, *Ultrason Sonochem.* **2015**, *22*, 371–381. http://dx.doi.org/10.1016/j.ultsonch.2014.05.023
22. Hafeezullah, Z. H. Yamani, J. Iqbal, A. Qurashi, A. Hakeem, *J. Alloys Compd*. **2014,** *616*, 76–80. http://dx.doi.org/10.1016/j.jallcom.2014.07.015
23. H. Xu, B. W. Zeiger, K. S. Suslick, *Chem. Soc. Rev.* **2013,** *42*, 2555–2567. http://dx.doi.org/10.1039/C2CS35282F
24. X. Wu, Z. Wei, L. Zhang, X. Wang, H. Yang, J. Jiang, *J. Nanomater.* **2014,** *2014*, 1–6.
25. V. Gandhi, R. Ganesan, H. H. A. Syedahamed, M. Thaiyan, *J. Phys. Chem. C* **2014,** *118*, 9715–9725. http://dx.doi.org/10.1021/jp411848t
26. Y. Rao, H. Xu, Y. Liang, S. Hark, *Cryst. Eng. Comm.* **2011**, *13*, 2566–2570. http://dx.doi.org/10.1039/c0ce00730g
27. J. Geng, G.-H. Song, J. -J. Zhu, *J. Nanomater.* **2012**, *2012*, 1–5.
28. B. Shahmoradi, K. Soga, S. Ananda, R. Somashekar, K. Byrappac, *Nanoscale* **2010**, *2*, 1160–1164. http://dx.doi.org/10.1039/c0nr00069h
29. S. Anandan, M. Miyauchi, *Phys. Chem. Chem. Phys*. **2011,** *13*, 14937–14945. http://dx.doi.org/10.1039/c1cp21514k

30. L. -W. Sun, H. -Q. Shi, W. -N. Li, H. -M. Xiao, S. -Y. Fu, X. -Z. Cao, Z. -X. Li, *J. Mater. Chem.* **2012,** *22*, 8221–8227. http://dx.doi.org/10.1039/c2jm00040g
31. Y. Liu, W. Luo, R. Li, G. Liu, M. R. Antonio, X. Chen, *J. Phys. Chem. C* **2008,** *112*, 686–694. http://dx.doi.org/10.1021/jp077001z
32. Y. Liu, K. Ai, Q. Yuan, L. Lu, *Biomaterials* **2011**, *32*, 1185–1192. http://dx.doi.org/10.1016/j.biomaterials.2010.10.022
33. J. Du, Z. Liu, Y. Huang, Y. Gao, B. Han, W. Li, G. Yang, *J. Cryst. Growth* **2005,** *280*, 126–134. http://dx.doi.org/10.1016/j.jcrysgro.2005.03.006
34. T. Thilagavathi, D. Geetha, *Appl. Nanosci.* **2014**, *4*, 127–132. http://dx.doi.org/10.1007/s13204-012-0183-8
35. R. S. Zeferino, M. B. Flores, U. Pal, *J. Appl. Phys.* **2011,** *109*, 014308(1–6).
36. A. K. Zak, W. H. A. Majid, M. E. Abrishami, R. Yousefi, *Solid State Sci.* **2011,** *13*, 251–256. http://dx.doi.org/10.1016/j.solidstatesciences.2010.11.024
37. S. Singhal, J. Kaur, T. Namgyal, R. Sharma, *Physica B* **2012,** *407,* 1223–1226. http://dx.doi.org/10.1016/j.physb.2012.01.103

Povzetek

S sonokemijsko metodo, pri kateri smo uporabili različne surfaktante (PVP/CTAB), smo sintetizirali ZnO in ZnO dopiran z Gd. Nanodelce smo karakterizirali s praškovno rentgensko difrakcijo (PXRD), infrardečo spektroskopijo (FTIR), vrstično elektronsko mikroskopijo (SEM), energijsko disperzivno rentgensko spektroskopijo (EDS) in UV-VIS spektroskopijo. Velikost delcev smo določili s tehniko dinamičnega sipanja svetlobe (DLS). Preučevali smo tudi vpliv Gd, kot dopirnega elementa in vpliv uporabljenega surfaktanta na velikost, morfologijo in optične lastnosti ZnO. Raziskovali smo tudi vpliv narave surfaktanta na množino Gd v mreži ZnO.